Research Square

Preprints are preliminary reports that have not undergone peer review.
They should not be considered conclusive, used to inform clinical practice,
or referenced by the media as validated information.

Silicon and Selenium nanoparticles synergistically alleviate arsenic toxicity and enhance chamomile (Matricaria chamomilla L.) yield and quality under drought stress

Afshin Nourizadeh
Lorestan University
Mahboobeh Jalali
Jalali.mah@lu.ac.ir
Lorestan University

Article

Keywords: Arsenic toxicity, Chamomile, Drought stress, Nanocomposite, Selenium nanoparticles, Silicon nanoparticles

Posted Date: September 11th, 2026

DOI: https://doi.org/10.21203/rs.3.rs-10691832/v1

License: This work is licensed under a Creative Commons Attribution 4.0 International License.
Read Full License

Additional Declarations: No competing interests reported.

Silicon and Selenium nanoparticles synergistically alleviate arsenic toxicity and enhance chamomile (*Matricaria chamomilla* L.) yield and quality under drought stress

Afshin Nourizadeh, Mahboobeh Jalali

Soil Sciences Department, Faculty of Agriculture, Lorestan University, Khorramabad, Iran, Jalali.mah@lu.ac.ir

Abstract

German chamomile (*Matricaria chamomilla* L.) faces threats from drought and arsenic contamination, which compromise its medicinal quality and yield. This study evaluated the combined application of silicon and selenium nanoparticles to counteract these stresses. A greenhouse factorial experiment was conducted with two irrigation levels (95% and 55% field capacity), two arsenic concentrations (0 and 50 mg kg^{-1}), and five nanoparticle regimes: control, SiNPs alone, SeNPs alone, a physical mixture (nSi+nSe), and a pre-synthesized silicon-selenium nanocomposite (nSi@nSe). Exposure to concurrent drought and arsenic stress diminished plant height, flower yield, chlorophyll content, essential oil percentage, and bioactive constituents like chamazulene and α-Bisabolol. It elevated oxidative stress markers, including malondialdehyde (MDA) and electrolyte leakage (EL), alongside increased phenol content and arsenic accumulation in roots and shoots. Among treatments, the nSi@nSe proved most effective. It reduced MDA by 46% and EL by 45% relative to the stressed control. Furthermore, it significantly curtailed arsenic uptake, lowering root concentrations from 23.2 to 15.5 mg kg^{-1} DW and shoot levels from 10.08 to 5 mg kg^{-1} DW, while decreasing the translocation factor from 0.45 to 0.32. This treatment boosted chamazulene and essential oil yields even under severe stress. nSi@nSe synergistically secures chamomile yield, safety, and medicinal integrity in contaminated droughts.

Keywords: Arsenic toxicity, Chamomile, Drought stress, Nanocomposite, Selenium nanoparticles, Silicon nanoparticles

1. Introduction

German chamomile (*Matricaria chamomilla* L.) is undeniably a high-value medicinal plant, but from my perspective as a soil chemist and plant nutritionist, its economic significance, rooted in the anti-inflammatory and antimicrobial compounds chamazulene and α-bisabolol is only half the story [1]. The

essential oil, which is produced and stored in the glandular trichomes of the flower heads, commands a high market price. However, the primary constraint in arid and semi-arid regions is not soil fertility or fertilizer management, but rather the availability of water. Drought doesn't just shrink yields; it directly impairs the biosynthesis of those very secondary metabolites that give the oil its value. So, for sustainable production, our focus as crop scientists must shift from chasing higher biomass to managing soil water-holding capacity and irrigation efficiency, because without addressing water stress, even the best-nourished chamomile plant will fail to deliver its chemical potential [2].

From a physiological standpoint, drought stress is a multifactorial inhibitor. It disrupts stomatal conductance. It also impairs mesophyll CO_2 diffusion. This reduces photosystem II efficiency. Consequently, net photosynthesis declines. Less biomass accumulates in reproductive organs. Terpenoid biosynthesis is also directly reduced [3, 4]. Water deficit triggers a specific stress response in chamomile. Chlorophyll degrades progressively [5]. Osmotic adjustment occurs via proline and glycine betaine accumulation. The essential oil chemoprofile also changes qualitatively [6]. Moderate stress can increase oil percentage on a dry-weight basis. This is a concentration effect. However, total flower biomass per plant decreases substantially. Net oil yield per unit area is significantly reduced. This has a negative impact on commercial viability.

Arsenic contamination adds another layer of complexity. This toxic metalloid enters the soil-plant system through various pathways. These include contaminated irrigation water and historical pesticide use. A critical pathway is the use of phosphate fertilizers. These fertilizers are derived from sedimentary apatite with high arsenic levels [7]. In soil, arsenic is mainly present as arsenate [As(V)]. It is a phosphate analog. It enters roots via high-affinity phosphate transporters. Arsenite [As(III)] enters through aquaglyceroporin channels [8]. Once inside, arsenic triggers a cascade of toxic effects. It uncouples oxidative phosphorylation. It competitively inhibits ATP and nucleic acid metabolism. Crucially, it generates reactive oxygen species via Fenton-type reactions. This leads to lipid peroxidation and protein carbonylation. Photosynthetic pigments are destroyed, compromising cellular integrity [9]. For chamomile, this creates a dual problem. Agronomic performance decreases. Product safety for human consumption is compromised. This is a serious concern for herbal preparations [7].

Drought and arsenic stress often co-occur. They frequently overlap in regions with water scarcity and industrial contamination. Critically, the combined effect is often synergistic. Plants show heightened sensitivity. Mitigation strategies must address both stressors and this requires effective and sustainable intervention approaches [10].

Nanotechnology offers a promising frontier. Nanoparticles have a high specific surface area. They exhibit unique physicochemical properties. Amorphous silicon dioxide and elemental selenium nanospheres have shown distinct stress-ameliorative properties [11]. Silicon nanoparticles (SiNPs) provide structural and biochemical protection. At the apoplastic level, SiNPs polymerize below the cuticle. This reinforces cell walls and reduces water loss. It also restricts the apoplastic flow of toxic metalloid cations. Silicon modulates aquaporin expression, sustaining root hydraulic conductivity. Biochemically, silicon primes the ascorbate-glutathione cycle and it enhances the redox buffering capacity. For heavy metals, SiNPs promote rhizospheric arsenic complexation. They reduce root-to-shoot translocation. They enhance vacuolar sequestration of arsenic [12].

Selenium nanoparticles (SeNPs) function differently. They are beneficial, though not essential, trace elements. Se acts as a cofactor for glutathione peroxidase-like activity. At optimal concentrations, SeNPs reduce oxidative stress markers like MDA and H_2O_2. They sustain photosystem II efficiency. They augment non-enzymatic antioxidants like phenolics and flavonoids. Also, SeNPs regulate phytohormonal crosstalk (auxin, gibberellin, ABA). This enhances stomatal sensitivity and overall stress resilience [13].

Combined nanoparticle application may yield synergistic benefits. Si and Se nanoparticles target multiple stress pathways simultaneously. Silicon provides a physical and structural shield. Selenium reinforces the biochemical antioxidant network. This creates a comprehensive defense phenotype. Research on synergistic effects in medicinal plants is limited. German chamomile is an ideal model system. It has a well-characterized secondary metabolome and economic sensitivity. Mechanistic understanding is essential for field-deployable strategies.
This study was designed to evaluate the individual and combined effects of silicon and selenium nanoparticles on mitigating arsenic toxicity, improving quantitative yield parameters, enhancing qualitative traits and modulating physiological and biochemical responses under drought stress, while rigorously testing the hypothesis that their synergistic application confers superior stress tolerance and offers a promising strategy for enhancing chamomile production in marginal environments.

2. Results

2.1. Characterization of SiNPs and SeNPs

Silicon nanoparticles used in this study were procured from Krangin Company (Iran). To verify particle size and purity, scanning electron microscopy (SEM) and energy-dispersive X-ray spectroscopy (EDS) analyses were performed at the Razi Metallurgy Research Institute (Fig. 1). The EDS spectrum confirmed the elemental composition of the nanoparticles as SiO_2, revealing two distinct sharp peaks in the 0–5 keV

region, corresponding to oxygen and silicon, respectively. SEM micrographs revealed relatively spherical nanoparticles with uniform size distribution on the surface. The average particle size was estimated to range between 8–10 nm, with a mean diameter of 8.3 nm.

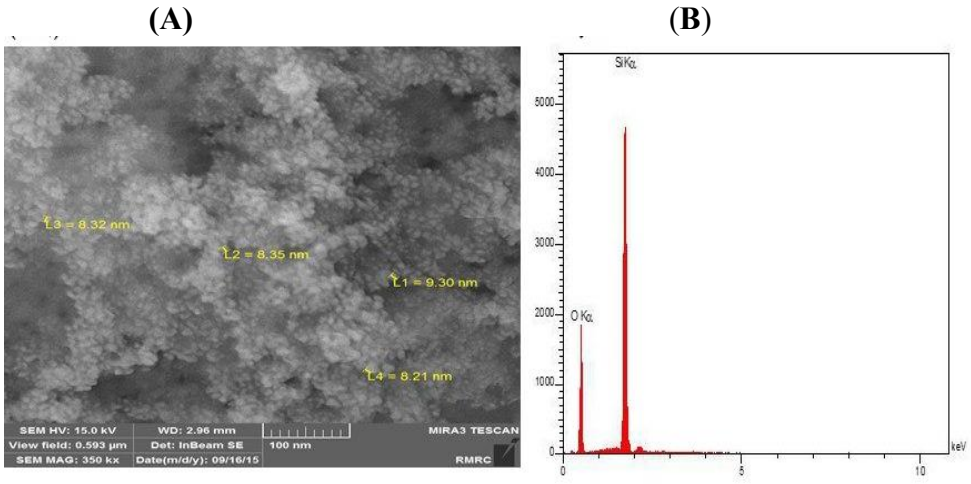


Fig. 1 Scanning electron microscopy (SEM) image (A) and energy-dispersive X-ray spectroscopy (EDS) spectrum (B) of SiNPs

Selenium nanoparticles were obtained from Pishgaman Nanomaterials Iranian Company (Fig 2). The nanoparticles exhibited the following characteristics: particle size range of 10–45 nm, bulk density of 3.89 g cm^{-3}, approximately spherical morphology, zeta potential of –32.8 mV, Z-average of 41.35 nm, and polydispersity index (PDI) of 0.565.

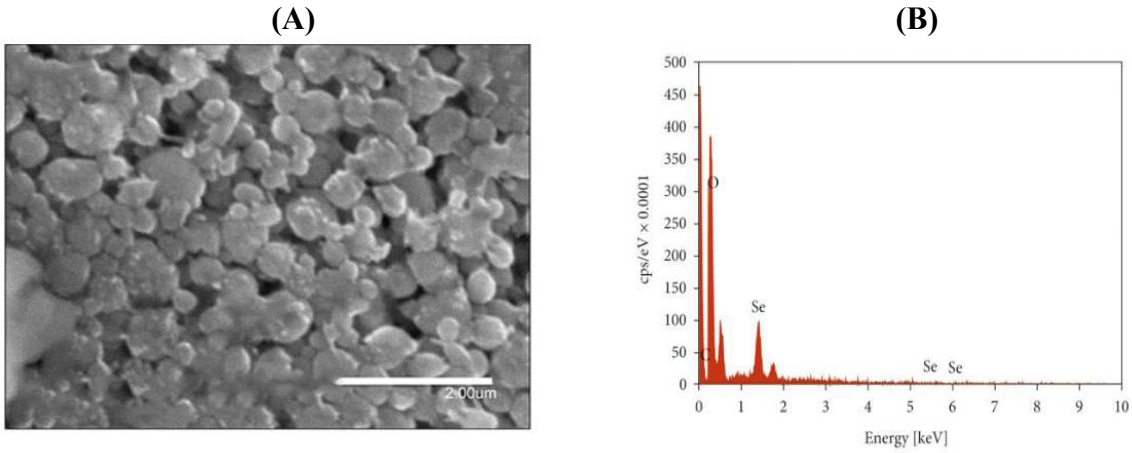


Fig. 2 Scanning electron microscopy (SEM) image (A) and energy-dispersive X-ray spectroscopy (EDS) spectrum (B) of SeNPs

2.2. Effect of SiNPs and SeNPs on morphologic parameters

The results of analysis of variance regarding the effects of different treatments on the morphological traits of chamomile plants showed that only the main effects were significant for plant height, capitulum diameter, number of lateral branches, and flower yield at the 1% probability level, while the interactive effects were not significant (Table 1).

Table 1 Variance analysis results of the effect of drought stress (D), arsenic (A), and nanoparticles (N) on morphologic parameters of *Matricaria chamomilla* L.

Source of variation	*df*	Plant Height	Capitulum diameter	Number of lateral branches per plant	Flower yield
D	1	17.36**	859.24*	3.48**	37593.70**
A	1	120.49**	55.091**	1.34**	23.98**
N	4	24.65**	76.31**	0.68**	414.54**
D*A	1	9.660 ns	15.88 ns	0.79 ns	45.93 ns
D*N	1	11.045 ns	38.43 ns	0.86 ns	27.89 ns
A*N	4	19.33 ns	48.3 ns	0.54 ns	256.41 ns
D*A*N	4	7.033 ns	23.69 ns	0.31 ns	168.34 ns
Residual	30	8.67	12.96	0.006	58.92
CV (%)	-	13.97	17.36	9.68	8.55

"*" and "**" indicate significant difference at levels of 5% and 1%, respectively, and " ns " indicates non-significant effect.

The mean comparison results indicated that both water deficit stress and arsenic stress significantly reduced plant height compared to the control treatment (Table 2). In contrast, the combined application of SiNPs and SeNPs, either as a nanocomposite or as a physical mixture, resulted in a significant increase in plant height relative to both the control treatment and the individual application of each nanoparticle. Furthermore, the evaluation of other traits, including capitulum diameter, number of lateral branches, and flower yield, revealed that water deficit and arsenic stresses caused significant reductions in these parameters (Table 3). The maximum values of capitulum diameter, lateral branch number, and flower yield were observed in Si@Se treatment.

Table 2 The main effects of drought stress (D), arsenic (A), and nanoparticles (N) on morphologic parameters of *Matricaria chamomilla* L.

	Plant height (cm)	capitulum diameter (cm)	Number of sub-branches	Flower yield (kg ha^{-1})
D				
D0	40.28± 1.25[a]	2.09 ± 0.03[a]	12.17± 0.12[a]	225.3± 10.85[a]
D1	37.87 ± 1.42[b]	1.53 ± 0.02[b]	8.83 ± 0.32[b]	160.4 ± 11.64[b]
A ($mgkg^{-1}$)				
A0	41.82 ± 1.13[a]	2.11 ± 0.01[a]	12.42± 0.25[a]	241.9± 15.25[a]
A1	38.42 ± 1.32[b]	1.74 ± 0.02[b]	9.96 ± 0.33[b]	173.6 ± 12.42[b]
N (mg kg^{-1})				
C	39. 5 ± 1.47[d]	2.01± 0.09[d]	11.03± 0.29[d]	236.7± 10.88[c]
nSi	45.61 ± 1.38[b]	2.48 ± 0.04[c]	12.15 ± 0.34[c]	295.4 ± 13.92[b]
nSe	44.75 ± 1.65[bc]	2.50 ± 0.01[b]	13.85 ± 0.14[b]	272.1± 14.66[b]
nSi+ nSe	46.93 ± 1.95[ab]	2.65 ± 0.01[b]	15.21 ± 0.51[ab]	315.4± 20.08[a]
nSi@nSe	48.4 ± 1.01[a]	2.83 ± 0.01[a]	16.4 ± 0.40[a]	330.7± 19.73[a]

Duncan's multiple range test (DMRT) indicates that there is no significant difference between the same letters at P≤0.05.

2.3. Effect of of SiNPs and SeNPs on physiological parameters

Analysis of variance revealed that drought stress (D), arsenic (A), and nanoparticles (N) had significant individual effects on most of the physiological parameters assessed in *Matricaria chamomilla* L (Table 4). Drought stress significantly influenced all measured traits, including total chlorophyll, total phenol, EL, MDA content, SOD activity, and RWC, at either 1% or 5% probability levels. Arsenic application also exhibited highly significant effects ($p < 0.01$) on all studied parameters. Furthermore, nanoparticle treatment significantly affected total chlorophyll, MDA content, SOD activity, and RWC, while its effect on total phenol was not significant. Among the two-way interactions, the D×A interaction was significant for total chlorophyll, total phenol, and EL; the D×N interaction was significant for total chlorophyll, total phenol, and EL; and the A×N interaction was significant for total chlorophyll and total phenol. The three-way interaction (D×A×N) was only significant for total chlorophyll and total phenol (Table 3).

Table 3: Variance analysis results of the effect of drought stress (D), arsenic (A), and nanoparticles (N) on physiological parameters of *Matricaria chamomilla* L.

Source of variation	*df*	RWC	SOD activity	MDA content	Electrolyte leakage	Total phenol	Total chlorophyll
D	1	17.36**	859.24*	3.48**	37593.70**	26.64*	8.71**

A	1	120.49**	55.091**	1.34**	23.98**	64.87**	899.6**
N	4	24.65**	76.31**	0.68**	414.54**	87.32 ns	7.04 **
D*A	1	9.660 ns	15.88 ns	0.79 ns	45.93 ns	10.54 **	2.28 **
D*N	1	11.045 ns	38.43 ns	0.86 ns	27.89 ns	12.65 *	0.62 **
A*N	4	19.33 ns	48.3 ns	0.54 ns	256.41 ns	9.76 **	1.7 **
D*A*N	4	7.033 ns	23.69 ns	0.31 ns	168.34 ns	5.87 **	2.85 *
Residual	30	8.67	12.96	0.006	58.92	0.97	0.26
CV (%)	-	13.97	17.36	9.68	8.55	11.76	2.11

"*" and "**" indicate significant difference at levels of 5% and 1%, respectively, and " ns " indicates non-significant effect.

The results showed that the highest percentage of RWC was observed at 95% FC without salinity stress in the treatment of nSi@nSe (59.4%) (Fig. 3). However, no significant difference was found between this treatment and the combined treatment of nSi+ nSe under both no-salinity and drought stress conditions. Exposure to arsenic alone (A1D0) or drought alone (A0D1) generally increased the values across treatments compared to the control condition, indicating stress-induced elevation of the parameter. Under combined arsenic and drought stress (A1D1), the highest values were observed, suggesting a synergistic exacerbation of stress effects (Figure 3).

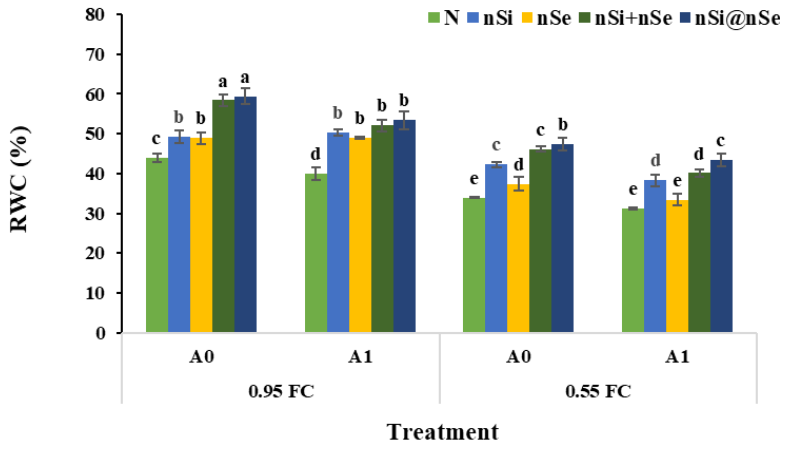


Fig. 3. The interplay between different treatments (drought stress (D), arsenic (A), and nanoparticles (N)) on the on RWC of *Matricaria chamomilla* L. Abbreviations: A0: no arsenic stress, A1: soil contaminated with 50 mg kg^{-1} arsenic; N: no nanoparticles, nSi: application of silicon nanoparticles, nSe: application of selenium nanoparticles, nSi+nSe: application of a mixture of silicon nanoparticles and selenium nanoparticles, nSi@nSe: application of a composite of silicon nanoparticles and selenium nanoparticles. DMRT indicates that there is no significant difference between the same letters at $p \leq 0.05$.

The results showed that, both drought and arsenic stresses increased SOD enzyme activity (Fig. 4). The highest activity of this enzyme was observed in the control treatment in soil contaminated with 50 mg kg-1 arsenic at 0.55 FC. Under non-stress conditions, no significant difference was observed among the different nanoparticle treatments, but as stress increased, this difference became more pronounced (Fig. 4).

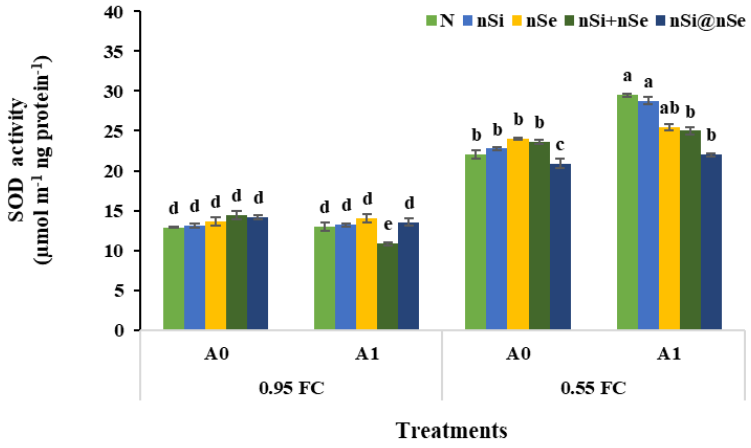


Fig 4. The interplay between different treatments (drought stress (D), arsenic (A), and nanoparticles (N)) on the on SOD activity of *Matricaria chamomilla* L. Abbreviations: A0: no arsenic stress, A1: soil contaminated with 50 mg kg^{-1} arsenic; N: no nanoparticles, nSi: application of silicon nanoparticles, nSe: application of selenium nanoparticles, nSi+nSe: application of a mixture of silicon nanoparticles and selenium nanoparticles, nSi@nSe: application of a composite of silicon nanoparticles and selenium nanoparticles. DMRT indicates that there is no significant difference between the same letters at $p \leq 0.05$.

Regarding the effect of different treatments on MDA content, the results showed that this trait increased with increasing stress (drought and arsenic) (Fig. 5). Under drought stress conditions (0.55% FC) and with the application of 50 mg kg-1 arsenic, the application of nSi@nSe reduced MDA content by 46% compared to the control treatment. Under non-stress conditions (A0D0), the lowest value was recorded in the nSi@nSe treatment (9.6 µg g-1FW), while the control showed the highest (14.6 µg g-1FW), indicating that nanoparticle application, particularly the nSi@nSe, effectively reduced stress-related parameters even in the absence of exogenous stressors. Exposure to arsenic alone (A1D0) or drought alone (A0D1) increased the measured values across all treatments compared to their respective non-stressed controls, with drought stress generally exerting a more pronounced effect than arsenic. The combined application of arsenic and drought (A1D1) resulted in the highest values, confirming a synergistic exacerbation of oxidative damage (Fig. 5).

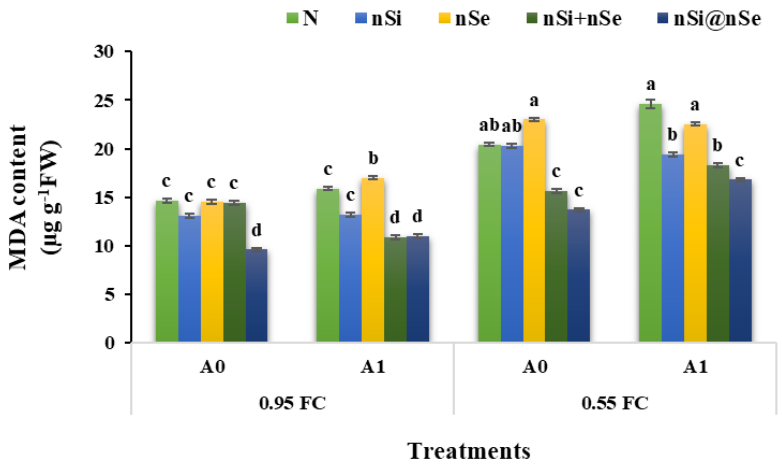


Fig. 5. The interplay between different treatments (drought stress (D), arsenic (A), and nanoparticles (N)) on the on MDA content of *Matricaria chamomilla* L. Abbreviations: A0: no arsenic stress, A1: soil contaminated with 50 mg kg^{-1} arsenic; N: no nanoparticles, nSi: application of silicon nanoparticles, nSe: application of selenium nanoparticles, nSi+nSe: application of a mixture of silicon nanoparticles and selenium nanoparticles, nSi@nSe: application of a composite of silicon nanoparticles and selenium nanoparticles. DMRT indicates that there is no significant difference between the same letters at $p \leq 0.05$.

The results regarding the effect of different treatments on EL showed that as drought stress increased, EL significantly increased across all treatments (Fig. 6). Arsenic contamination also led to an increase in EL. The highest value of this trait (62.3%) was observed in the control treatment under 0.55% FC with the application of 50 mg kg^{-1} arsenic, while the lowest value (17.2%) was recorded in the treatment with nano-silicon application under 0.95% FC and without arsenic stress (Fig. 6).

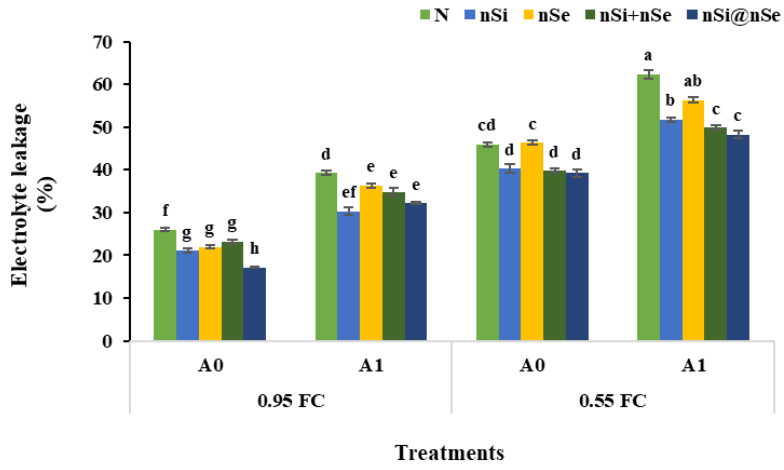


Fig. 6. The interplay between different treatments (drought stress (D), arsenic (A), and nanoparticles (N)) on the on EL of *Matricaria chamomilla* L. Abbreviations: A0: no arsenic stress, A1: soil contaminated with 50 mg kg^{-1} arsenic; N: no nanoparticles, nSi: application of silicon nanoparticles, nSe: application of selenium nanoparticles, nSi+nSe: application of a mixture of silicon nanoparticles and selenium nanoparticles, nSi@nSe:

application of a composite of silicon nanoparticles and selenium nanoparticles. DMRT indicates that there is no significant difference between the same letters at $p \leq 0.05$.

Comparison of the mean data showed that with increasing drought and arsenic stress, total phenol content significantly increased across all treatments (Fig. 7). Under the combined condition of drought stress and arsenic stress (0.55% FC A1), no significant differences were observed among the various treatments.

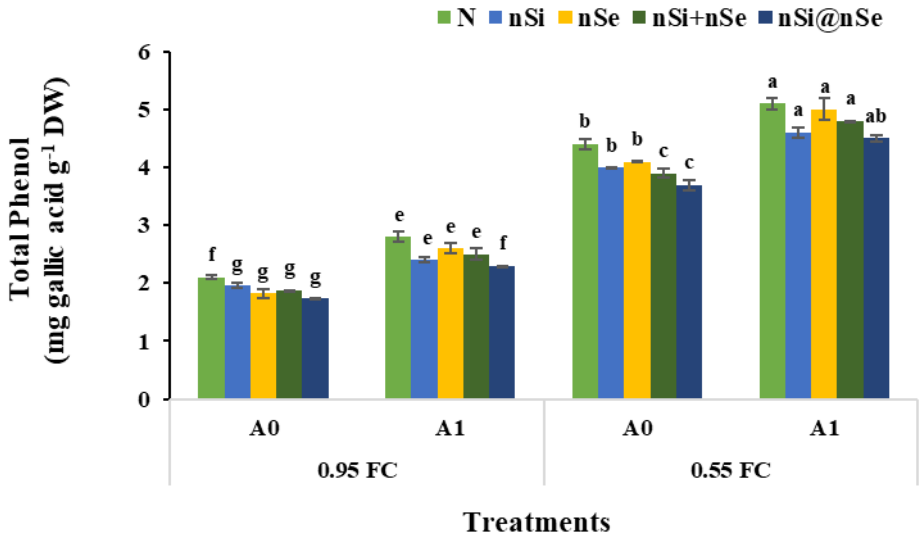


Fig. 7. The interplay between different treatments (drought stress (D), arsenic (A), and nanoparticles (N)) on the on total phenol of *Matricaria chamomilla* L. Abbreviations: A0: no arsenic stress, A1: soil contaminated with 50 mg kg^{-1} arsenic; N: no nanoparticles, nSi: application of silicon nanoparticles, nSe: application of selenium nanoparticles, nSi+nSe: application of a mixture of silicon nanoparticles and selenium nanoparticles, nSi@nSe: application of a composite of silicon nanoparticles and selenium nanoparticles. DMRT indicates that there is no significant difference between the same letters at $p \leq 0.05$.

The comparison of mean values revealed that with increasing drought stress, leaf chlorophyll content decreased significantly (Fig. 7). The highest SPAD content was observed under the combined application of silicon and selenium nanoparticles, whether in the form of a composite or as a physical mixture. Conversely, the lowest chlorophyll content was recorded in the control treatment under drought stress at 0.55 FC, with the addition of 50 mg kg-1 arsenic.

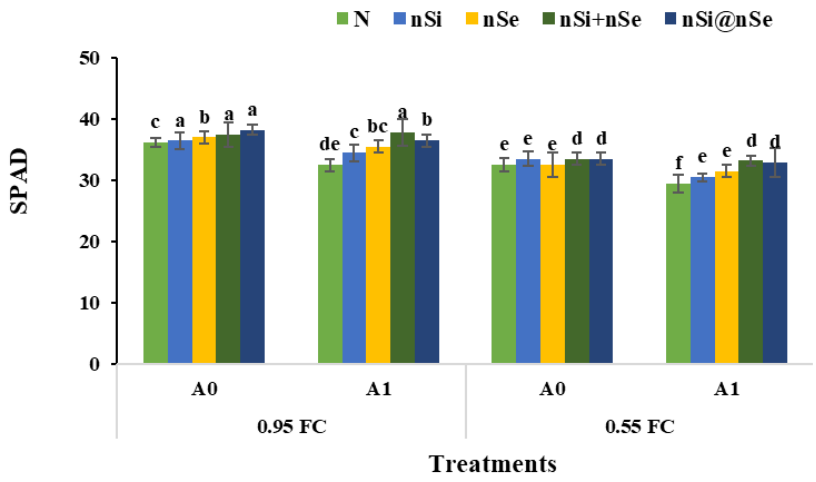


Fig 7. The interplay between different treatments (drought stress (D), arsenic (A), and nanoparticles (N)) on the on chlorophyll content of *Matricaria chamomilla* L. Abbreviations: A0: no arsenic stress, A1: soil contaminated with 50 mg kg^{-1} arsenic; N: no nanoparticles, nSi: application of silicon nanoparticles, nSe: application of selenium nanoparticles, nSi+nSe: application of a mixture of silicon nanoparticles and selenium nanoparticles, nSi@nSe: application of a composite of silicon nanoparticles and selenium nanoparticles. DMRT indicates that there is no significant difference between the same letters at $p \leq 0.05$.

2.4. Effect of SiNPs and SeNPs on the quantity and quality of essential oil, root and shoot arsenic of *Matricaria chamomilla* L.

The ANOVA results revealed that drought stress (D), arsenic (A), and nanoparticles (N) each significantly influenced essential oil content, chamazulene, α-bisabolol, and arsenic accumulation in chamomile ($p < 0.01$ for most traits). The two-way interactions (D×A, D×N, and A×N) were significant for the majority of parameters, indicating that the effect of one factor is modulated by the level of another, though α-bisabolol showed non-significant responses in several interactions. The three-way interaction (D×A×N) was significant for all traits except α-bisabolol, demonstrating that the combined effects of these three factors are highly interdependent and context-dependent. This implies that the effectiveness of silicon and selenium nanoparticles in improving essential oil quality and reducing arsenic uptake varies with drought intensity and arsenic concentration (Table 4).

Table 4: Variance analysis results of the effect of drought stress (D), arsenic (A), and nanoparticles (N) the quantity and quality of essential oil, root and shoot arsenic of of *Matricaria chamomilla* L.

Source of variation	*df*	Essential oil	Chamazulene	α-Bisabolol	Root arsenic	Shoot arsenic	Arsenic translocation factor
D	1	8.71**	552.9**	428.06**	2754.87**	8642.42*	257.64*
A	1	899.6**	279.86**	1432.35**	4362.4**	3265.02**	262.87**
N	4	7.04**	314.3**	3621.6**	9737.23**	547.84*	175.76*
D*A	1	2.28**	232.6**	425.39^{ns}	308.11**	278.33**	342.65**
D*N	1	0.62**	962.45**	315.8^{ns}	763.54**	631.7^{ns}	37.9^{ns}
A*N	4	1.7^{ns}	521.2**	315.53^{ns}	14.98**	673.84**	507.44**
D*A*N	4	2.85**	121.4**	24.88^{ns}	43.76**	641.5*	24.97*
Residual	30	0.26	5.63	3.83	4.09	9.35	5.87
CV (%)	-	14.86	18.12	6.94	5.92	11.53	13.07

"*" and "**" indicate significant difference at levels of 5% and 1%, respectively, and " ns " indicates non-significant effect.

Essential oil content decreased significantly with increasing drought stress across all treatments (Fig. 8). The maximum essential oil content (0.89%) was obtained in the nSi@nSe treatment under 0.95 FC and in the absence of arsenic stress. In contrast, the minimum essential oil content was recorded in the control treatment under drought stress (0.55 FC) combined with 50 mg kg^{-1} arsenic application. Also, no significant differences were observed between the nSi@nSe and nSi+nSe treatments under any of the tested conditions (Fig. 8).

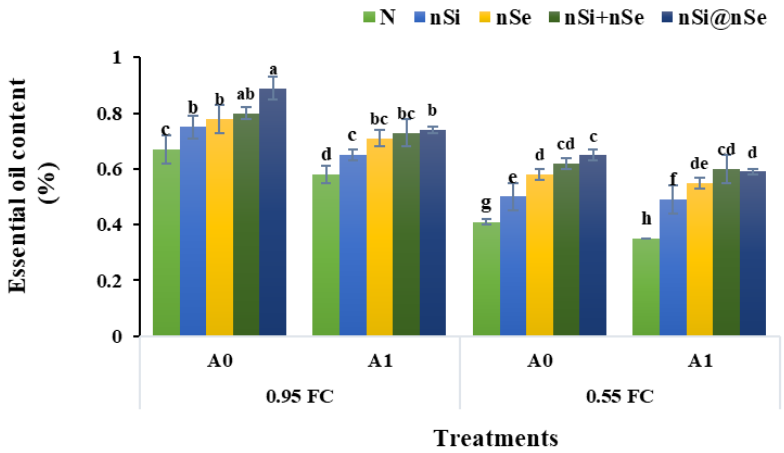


Fig 8. The interplay between different treatments (drought stress (D), arsenic (A), and nanoparticles (N)) on the on essential oil content of *Matricaria chamomilla* L. Abbreviations: A0: no arsenic stress, A1: soil contaminated with 50 mg kg^{-1} arsenic; N: no nanoparticles, nSi: application of silicon nanoparticles, nSe: application of selenium nanoparticles, nSi+nSe: application of a mixture of silicon nanoparticles and selenium nanoparticles, nSi@nSe: application of a composite of silicon nanoparticles and selenium nanoparticles. DMRT indicates that there is no significant difference between the same letters at $p \leq 0.05$.

Chamazulene content decreased significantly under drought and arsenic stress, with the lowest values observed under combined stress (A1D1), indicating stress-induced suppression of essential oil quality. Arsenic alone (A1D0) slightly reduced chamazulene, while drought alone (A0D1) caused a more pronounced decrease. The combined stress (A1D1) resulted in the lowest values across all treatments (Fig. 9).

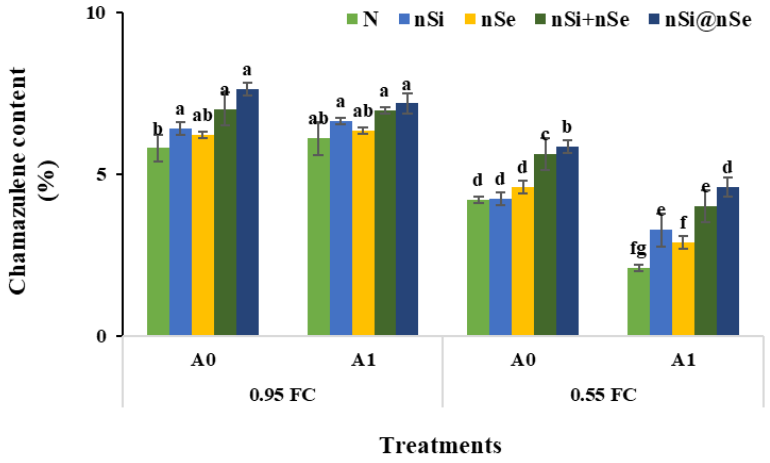


Fig 9. The interplay between different treatments (drought stress (D), arsenic (A), and nanoparticles (N)) on the on chamazulene content of *Matricaria chamomilla* L. Abbreviations: A0: no arsenic stress, A1: soil contaminated with 50 mg kg^{-1} arsenic; N: no nanoparticles, nSi: application of silicon nanoparticles, nSe: application of selenium nanoparticles, nSi+nSe: application of a mixture of silicon nanoparticles and selenium nanoparticles, nSi@nSe: application of a composite of silicon nanoparticles and selenium nanoparticles. DMRT indicates that there is no significant difference between the same letters at $p \leq 0.05$.

The results showed that the highest α-bisabolol content was observed in the nSi@nSe treatment under non-stress conditions (no drought and no arsenic stress), though this value was not significantly different from that of the nSi+nSe treatment under the same conditions. Overall, α-bisabolol content decreased significantly with increasing drought and arsenic stress levels. The lowest α-bisabolol content was recorded in the control treatment under 0.55 FC with the application of 50 mg kg^{-1} as sodium arsenate (Fig. 10).

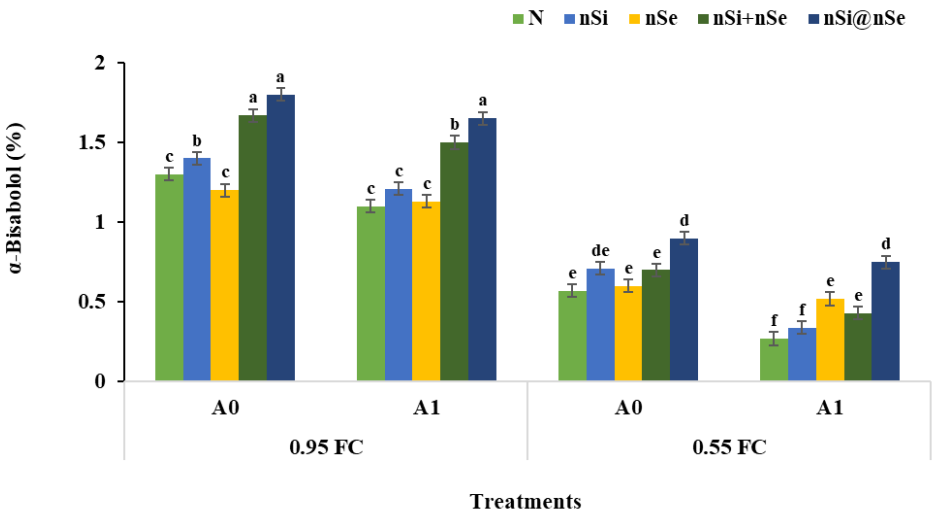


Fig. 10. The interplay between different treatments (drought stress (D), arsenic (A), and nanoparticles (N)) on the on α-Bisabolol of *Matricaria chamomilla* L. Abbreviations: A0: no arsenic stress, A1: soil contaminated with 50 mg kg^{-1} arsenic; N: no nanoparticles, nSi: application of silicon nanoparticles, nSe: application of selenium nanoparticles, nSi+nSe: application of a mixture of silicon nanoparticles and selenium nanoparticles, nSi@nSe: application of a composite of silicon nanoparticles and selenium nanoparticles. DMRT indicates that there is no significant difference between the same letters at $p \leq 0.05$.

Shoot arsenic concentration increased significantly under arsenic stress, with the highest values observed under combined drought and arsenic stress (A1D1), indicating that water deficit enhanced arsenic uptake and translocation to aerial parts (Fig 11). Under arsenic contamination alone (A1D0), arsenic accumulation ranged from 3.9 (nSi) to 5.3 (Control), while the combined stress (A1D1) led to substantially higher concentrations. The physical mixture (nSi+nSe) also performed better than individual applications, demonstrating a synergistic effect in reducing arsenic uptake. Silicon nanoparticles were more effective than nSe in limiting arsenic translocation, likely due to silicon's role in reinforcing cell walls and reducing apoplastic transport of toxic metalloids.

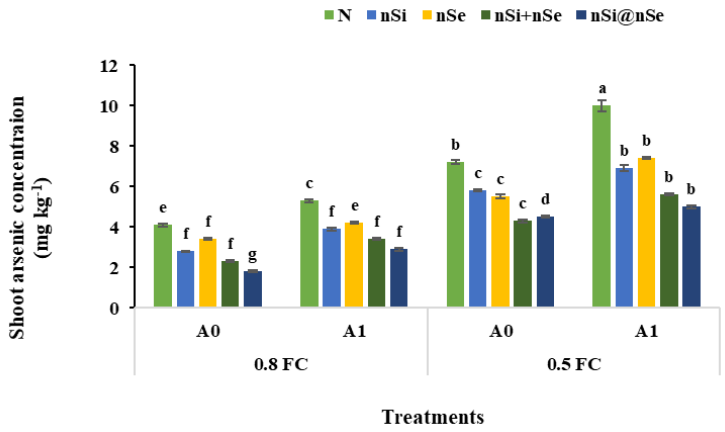
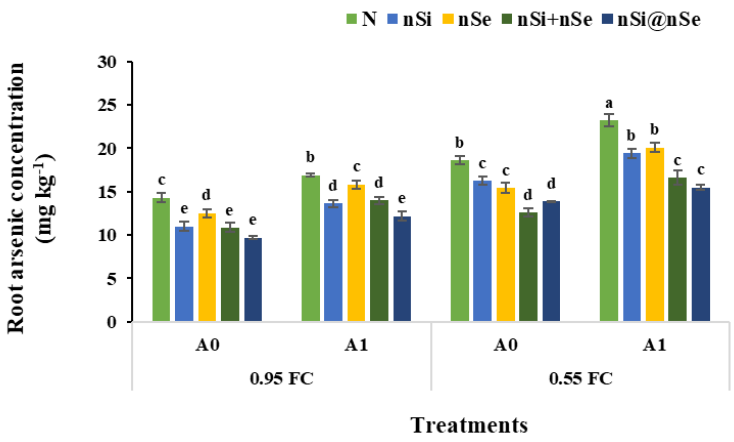


Fig 11. The interplay between different treatments (drought stress (D), arsenic (A), and nanoparticles (N)) on the on shoot arsenic concentration of *Matricaria chamomilla* L. Abbreviations: A0: no arsenic stress, A1: soil contaminated with 50 mg kg^{-1} arsenic; N: no nanoparticles, nSi: application of silicon nanoparticles, nSe: application of selenium nanoparticles, nSi+nSe: application of a mixture of silicon nanoparticles and selenium nanoparticles, nSi@nSe: application of a composite of silicon nanoparticles and selenium nanoparticles. DMRT indicates that there is no significant difference between the same letters at $p \leq 0.05$.

Root arsenic concentration increased significantly under arsenic stress, with the highest values observed under combined drought and arsenic stress (A1D1), indicating that water deficit enhanced arsenic uptake and accumulation in root tissues. Under arsenic contamination alone (A1D0), root arsenic ranged from 10.8 (nSi@nSe) to 17.0 (Control), while combined stress (A1D1) led to substantially higher concentrations, reaching up to 22.0 in the control treatment. Among nanoparticle treatments, the nanocomposite (nSi@nSe) consistently showed the lowest root arsenic accumulation under all stress conditions (16.0 under A1D1), followed by nSi (19.0) and nSe (18.0), while the physical mixture (nSi+nSe) performed better than individual applications (17.0). Silicon nanoparticles (nSi) were more effective than nSe in reducing arsenic accumulation in roots, likely due to silicon's role in reinforcing cell walls and limiting apoplastic transport of toxic metalloids. The synergistic effect of the nanocomposite highlights its potential as an effective strategy for reducing arsenic uptake and enhancing plant tolerance to heavy metal contamination.



328

329 **Fig 12.** The interplay between different treatments (drought stress (D), arsenic (A), and nanoparticles (N)) on the on
330 root arsenic concentration of *Matricaria chamomilla* L. Abbreviations: A0: no arsenic stress, A1: soil contaminated
331 with 50 mg kg^{-1} arsenic; N: no nanoparticles, nSi: application of silicon nanoparticles, nSe: application of selenium
332 nanoparticles, nSi+nSe: application of a mixture of silicon nanoparticles and selenium nanoparticles, nSi@nSe:
333 application of a composite of silicon nanoparticles and selenium nanoparticles. DMRT indicates that there is no
334 significant difference between the same letters at $p \leq 0.05$.

335

336 The translocation factor (TF) values were consistently below 1.0 across all treatments, indicating that
337 arsenic was predominantly retained in root tissues and limited translocation to aerial parts occurred. Under
338 non-stress conditions (A0D0), TF ranged from 0.19 (nSi@nSe) to 0.28 (Control). The combined application
339 of drought and arsenic (A1D1) led to the highest TF values (0.32–0.45), suggesting that water deficit
340 enhanced arsenic mobility from roots to shoots (Fig 13).

341

342

343

344

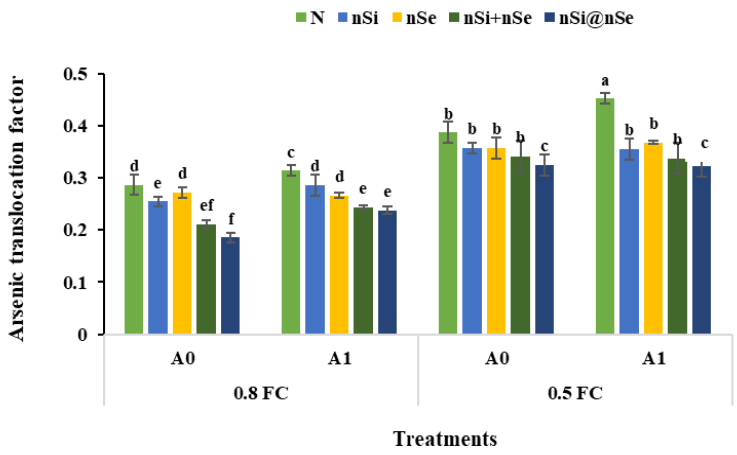


Fig 13. The interplay between different treatments (drought stress (D), arsenic (A), and nanoparticles (N)) on the on arsenic translocation factor of *Matricaria chamomilla* L. Abbreviations: A0: no arsenic stress, A1: soil contaminated with 50 mg kg^{-1} arsenic; N: no nanoparticles, nSi: application of silicon nanoparticles, nSe: application of selenium nanoparticles, nSi+nSe: application of a mixture of silicon nanoparticles and selenium nanoparticles, nSi@nSe: application of a composite of silicon nanoparticles and selenium nanoparticles. DMRT indicates that there is no significant difference between the same letters at $p \leq 0.05$.

3. Discussion

The findings of the present study provide compelling evidence for the synergistic protective effects of SiNPs and SeNPs, particularly as a nanocomposite (nSi@nSe), in alleviating the detrimental impacts of arsenic toxicity and drought stress on German chamomile (*Matricaria chamomilla* L.). The observed improvements in morphological, physiological, biochemical, and quality-related parameters underscore the complementary mechanisms through which these two beneficial elements operate.

A key finding of this study was the significant reduction in MDA content and EL in plants treated with nSi@nSe under combined drought and arsenic stress. These parameters serve as reliable indicators of lipid peroxidation and membrane damage, which are exacerbated by reactive oxygen species (ROS) generated under stress conditions [13]. The 46% reduction in MDA content and the consistently lower EL values in the nSi@nSe treatment compared to the control highlight its superior capacity to preserve membrane integrity. This synergistic effect can be attributed to the dual action of silicon and selenium. Silicon reinforces cell wall structure and reduces apoplastic transport of toxic metalloids, while selenium acts as a cofactor for glutathione peroxidase (GSH-Px), enhancing the detoxification of ROS. The enhanced activity of antioxidant enzymes, such as SOD observed in this study further corroborates the role of these nanoparticles in bolstering the plant's redox buffering capacity [14]. The superior performance of the nSi@nSe over individual or mixed applications suggests that the intimate association of Si and Se in the nSi@nSe facilitates more efficient delivery and synergistic interaction at the cellular level [15].

The study demonstrated that the application of nSi@nSe significantly reduced arsenic accumulation in both roots and shoots, while also minimizing the translocation factor. These findings are consistent with the known role of silicon in restricting the apoplastic movement of metalloids. Silicon promotes the complexation of arsenic in the rhizosphere and enhances its sequestration in root vacuoles, thereby limiting its transport to aerial parts [16]. The foliar application of chitosan-based silicon nanoparticles has been shown to reduce arsenic concentration in rice grains by promoting its attachment to leaf cell walls [17]. In our study, the nanocomposite's effectiveness in reducing TF values, particularly under combined stress, suggests that the presence of Se may augment silicon's effect by modulating the expression of Si transporters (e.g., Lsi1, Lsi2) involved in arsenic uptake. This is particularly important for chamomile, as reduced arsenic accumulation in flowers is crucial for ensuring the safety of herbal products for human consumption [18].

The decline in total chlorophyll content under stress was mitigated by the application of nanoparticles, with the nSi@nSe showing the best preservation. This aligns with studies showing that both Si and Se can sustain photosystem II efficiency and protect photosynthetic pigments from degradation under heavy metal and drought stress [19]. The maintenance of chlorophyll levels is vital for sustaining net photosynthesis and biomass production, which is reflected in the improved flower yield observed in this study.

Furthermore, the nanocomposite treatment significantly enhanced the content of chamazulene, the key bioactive compound in chamomile essential oil. While stress often suppresses terpenoid biosynthesis, the application of nSi@nSe appeared to counteract this effect, likely by reducing oxidative stress and maintaining metabolic flux toward secondary metabolite production. Selenium has been shown to enhance the biosynthesis of phenolic and flavonoid compounds by upregulating the phenylpropanoid pathway, and Si may contribute by improving overall plant health and nutrient status [20]. The increase in chamazulene content under combined stress is particularly noteworthy, as it demonstrates the nanoparticles' role in not only protecting the plant but also improving the quality of the harvested product. This is consistent with findings that bio-priming can enhance chamazulene percentage in chamomile under stress conditions [21].

The results of this study provide a strong scientific basis for the use of nSi@nSe as a sustainable strategy to enhance crop resilience in challenging environments. The synergistic effects observed are likely due to the complementary functions of silicon (physical barrier, structural support) and Se (biochemical antioxidant defense) [22]. This dual mechanism creates a robust defense phenotype that is more effective than either element alone. The use of nanotechnology to deliver these elements offers advantages in terms of targeted application and enhanced bioavailability. Future research should focus on elucidating the molecular mechanisms underlying this synergy, particularly the role of Si and Se in regulating stress-

responsive genes and phytohormonal crosstalk [13]. Field-scale trials are also necessary to validate the efficacy of this approach under real-world conditions and to optimize application rates for different crops and stress scenarios [23].

4. Materials and Methods

4.1. Experimental Design and Treatments

This research was conducted to investigate the alleviation of arsenic uptake risk in German chamomile (*Matricaria chamomilla* L.) using (SiNPs) and (SeNPs) under deficit irrigation conditions. The experiment was carried out at the Faculty of Agriculture, Lorestan University, located on the Khorramabad (longitude 48°22′ E, latitude 33°29′ N, altitude 1125 m above sea level), Iran, during the year 2025 (Fig. 14).

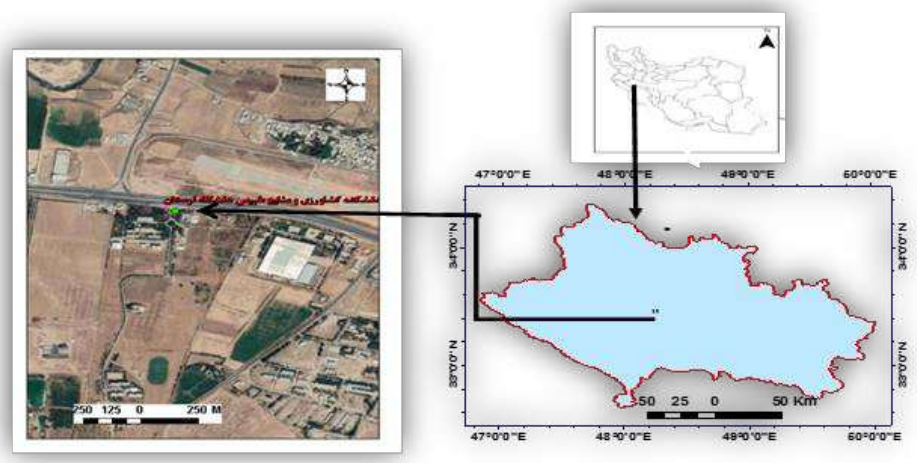


Fig 14. Geographical location of the research implementation site

The experiment was conducted as a completely randomized factorial design with three replications under controlled greenhouse conditions, incorporating three principal factors evaluated across multiple levels to comprehensively assess all treatment interactions. The first factor consisted of five nanoparticle treatments, which included a control with no nanoparticles (Control), SiNPs applied alone (nSi), SeNPs applied alone (nSe), a simple physical mixture of silicon and selenium nanoparticles (nSi+nSe), and a pre-synthesized silicon-selenium nanocomposite (Si@Se), with the remaining treatments serving as additional verification points. The second factor comprised two irrigation regimes, specifically a well-watered control maintained

at 95–100% of field capacity (FC) (D0), drought stress set at 55% of FC (D1). The third factor involved two arsenic levels, namely a control with no added arsenic (A0) and a contaminated treatment receiving 50 mg kg^{-1} arsenic supplied as sodium arsenate (A1).

Soil samples were collected from a depth of 0–30 cm at the Faculty of Agriculture, air-dried, and passed through a 2 mm sieve. The physicochemical properties of the soil were determined using standard methods [24] and are summarized in Table 5.

Table 5. Soil physical and chemical properties used in this assay

Soil parameter	Unit	Value
Soil texture	-	Clay loam
EC_e	dS m^{-1}	1.24
pH	-	7.72
FC	%	32.37
CEC	$Cmol^{+}$ kg^{-1} dry soil	27.3
Organic Carbon	%	0.68
$CaCO_3$	(%)	8.20
Olsen P	mg kg^{-1}	3.65
Available K	mg kg^{-1}	342
DTPA extractable Fe	mg kg^{-1}	3.8
DTPA extractable Zn	mg kg^{-1}	1.4
DTPA extractable Mn	mg kg^{-1}	11
Available arsenic	mg kg^{-1}	Nd*
Available selenium	mg kg^{-1}	Nd*
Total arsenic	mg kg^{-1}	<0.1
Total selenium	mg kg^{-1}	0.32

*Nd: Below detection limit of the instrument

To establish the experimental contamination regime, a predetermined quantity of sodium arsenate heptahydrate ($AsHNa_2O_4.7H_2O$) was dissolved in deionized water to yield a nominal arsenic concentration of 50 mg kg^{-1} on a dry-weight soil basis. The resulting arsenical solution was applied to the bulk soil matrix via uniform atomized spraying, following the protocol delineated by Hassani et al. and Mansouri et al. [25, 26]. Following application, the spiked soil was air-dried under controlled conditions, after which it was mechanically homogenized to ensure optimal spatial distribution of the contaminant. Subsequently, the contaminated substrate was combined with the uncontaminated potting soil in proportions corresponding to each treatment replicate, with iterative and rigorous mixing employed to guarantee macroscopic homogeneity across all experimental units. To facilitate physicochemical equilibration and allow for the stabilization of arsenic species within the soil matrix, the moisture content of the amended soil was adjusted

to field capacity and maintained under ambient conditions for a two-week aging period prior to the sowing of test specimens.

Each experimental unit consisted of a plastic pot (equipped with basal drainage apertures) containing 5.0 kg of air-dried sieved soil. Five seeds of Matricaria chamomilla L. were sown per pot at a uniform depth; following successful germination and seedling establishment, the stand was manually thinned to two uniform plants per pot to ensure consistent growth conditions and minimize intraspecific competition.

The plants were cultivated over a four-week establishment phase within a controlled greenhouse environment, maintained at a diurnal temperature regimen of 25 ± 2 °C, relative humidity ranging between 50–60 %, and a photoperiod of 16 h light: 8 h dark. Irrigation during this initial phase was managed gravimetrically: each pot was initially weighed to obtain the baseline pot-plus-soil mass. To determine FC, pots were saturated with tap water until free drainage commenced, then covered with impermeable plastic sheeting to preclude evaporative losses. After cessation of gravitational drainage, the pots were reweighed, and the gravimetric water content calculated on an oven-dry soil mass basis was designated as 100 % field capacity, following the protocol of Pourmansour et al. [27]. Throughout the first four weeks, all pots were irrigated daily to maintain soil moisture at 100 % FC, with water additions adjusted based on daily weight measurements.

At the commencement of the fifth week post-sowing, a differential irrigation regime was imposed to induce water deficit stress: the drought-stressed cohort was maintained at 50 % FC, while control pots continued at 100 % FC. Concurrently, nanoparticle suspensions were applied as foliar sprays using a manual hand-held atomizer until the point of visible runoff, administered on two separate occasions (specifically, during the first and third weeks of the fifth week). Control plants received an equivalent volume of distilled water via the same application method to standardize mechanical effects. Both arsenic contamination (established prior to planting) and the combined drought/nanoparticle treatments were sustained throughout a six-week stress period, terminating at the onset of full flowering phenological stage, at which point all plant material was harvested for subsequent physiological and biochemical analyses.

4.2. Measurements

At 100 days following sowing, corresponding to the full flowering stage, all experimental plants were destructively harvested for subsequent analyses. Upon collection, a suite of key morphological parameters was recorded to evaluate the integrative effects of the imposed treatments on plant development. Specifically, the following traits were quantified for each individual plant.

4.2.1. chlorophyll content index (SPAD)

Chlorophyll content was measured using a portable SPAD-502 chlorophyll meter (Konica Minolta, Japan), which determines relative chlorophyll concentration by measuring the transmittance of light through the leaf at wavelengths of 650 nm (red, absorbed by chlorophyll) and 940 nm (near-infrared, used as a reference). Measurements were taken on fully expanded, healthy leaves from the middle portion of each plant, avoiding the main veins to ensure consistency. Three readings per leaf were recorded from three randomly selected leaves per plant, and the average value was calculated and expressed in SPAD units.

4.2.2. Relative Water Content (RWC)

Leaf relative water content was measured according to Hanson and Hitz. [28]. Fresh leaves were weighed (FW), then floated on distilled water for 24 h. The turgid weight (TW) was recorded, and samples were oven-dried at 80°C for 48 h to determine dry weight (DW). RWC was calculated as:

$$RWC\ (\%) = [(FW - DW) / (TW - DW)] \times 100$$

4.2.3. Electrolyte Leakage (EL)

Electrolyte leakage was determined following Lutts et al. [29]. Leaf samples were washed with distilled water and placed in glass tubes containing 10 mL distilled water. After 24 h, electrical conductivity (EC_1) was measured. The tubes were then autoclaved at 120°C for 20 min, and after cooling, EC_2 was recorded. Electrolyte leakage percentage was calculated as:

$$EL\ (\%) = (EC_1 / EC_2) \times 100$$

4.2.4. Malondialdehyde (MDA) content

MDA content, an indicator of lipid peroxidation, was measured by homogenizing 0.5 g of fresh leaf tissue in 20% trichloroacetic acid (TCA) containing 0.5% thiobarbituric acid (TBA). The homogenate was heated at 95 °C for 25 min, cooled, and centrifuged, and absorbance was measured at 532 nm following Heath and Packer. [30].

4.2.5. Superoxide Dismutase (SOD) Activity Assay

Superoxide dismutase (SOD; EC 1.15.1.1) activity was measured based on its ability to inhibit the photochemical reduction of nitro blue tetrazolium (NBT). Fresh leaf tissue (0.3 g) was homogenized in cold phosphate buffer (50 mM, pH 7.8) containing 0.1 mM EDTA and centrifuged at 10,000 rpm for 15 minutes at 4°C. The reaction mixture (3 mL), containing 50 mM phosphate buffer (pH 7.8), 13 mM methionine, 75 µM NBT, 0.1 mM EDTA, 2 µM riboflavin, and 100 µL of enzyme extract, was illuminated under fluorescent light for 15 minutes. Absorbance was then measured at 560 nm. One unit of SOD activity was

505 defined as the amount of enzyme required to inhibit 50% of NBT photoreduction, and activity was
506 expressed as U mg^{-1} protein [31].

507 **4.2.6. Total Phenolic Content**

508 Total phenolic content was determined using the Folin–Ciocalteu method [32]. Fresh leaf tissue (0.5 g) was
509 ground in liquid nitrogen and extracted with 3 mL of 85% methanol. The extract was centrifuged at 10,000
510 rpm for 20 min at 4°C. Then, 10 µL of the supernatant was mixed with 50 µL of Folin–Ciocalteu reagent
511 and 580 µL of distilled water. After 5–8 min, 150 µL of 1 M sodium carbonate was added. The mixture
512 was incubated in darkness for 30 min at 40°C, and absorbance was measured at 765 nm. A blank was
513 prepared using 80% methanol instead of the extract.

514 **4.2.7. Arsenic concentrations of Shoot and Root**

515 Arsenic concentrations were analyzed following wet digestion [33]. Dried and powdered plant samples (0.5
516 g) were digested in a mixture of concentrated HNO_3 and $HClO_4$ (2:1 v/v) on a hot plate. After cooling, the
517 digests were dissolved in 2 mL of 10% HCl and diluted to 50 mL with distilled water. The resulting
518 solutions were used for determination of arsenic. Arsenic concentrations in the digested samples were
519 measured using inductively coupled plasma optical emission spectrometry (ICP-OES).

520 **4.2.8. Translocation Factors**

521 The translocation factor (TF) was calculated to determine the plant's ability to translocate arsenic from roots
522 to shoots [34].

523 TF = [As concentration in shoot] / [As concentration in root]

524

525 **4.2.9. Essential Oil Extraction and Analysis**

526 Essential oil was extracted from dried chamomile flowers by hydrodistillation using a Clevenger-type
527 apparatus (European Pharmacopoeia, 1996). Dried plant material (100 g) was slightly ground and placed
528 in the distillation flask with 800 mL distilled water, followed by heating for 3 h after boiling commenced.
529 The essential oil was collected in graduated tubes, and after volume measurement, the oil was separated
530 and dehydrated over anhydrous sodium sulfate. The essential oil samples were stored in amber glass vials
531 at 4°C in darkness for further analysis.

532 GC-MS Analysis: Gas chromatography (GC) and gas chromatography–mass spectrometry (GC-MS)
533 analyses were performed at the Chemistry Laboratory of the Research Institute of Forests and Rangelands,
534 Iran. The essential oil samples (1 µL diluted in 2 mL dichloromethane) were injected into the GC and GC-
535 MS systems.

4.3. Statistical Analysis

All data were subjected to analysis of variance (ANOVA) using SAS software (Version 9.4). Prior to ANOVA, normality of data distribution was assessed using the Kolmogorov–Smirnov test, and homogeneity of variances was confirmed using Levene's test. Main effects and interaction effects were evaluated using two-way ANOVA at a significance level of $\alpha = 0.05$. When significant, means were separated using Duncan's multiple range test at $P \leq 0.05$.

Ethics approval and consent to participate

Not applicable.

Consent for publication

Not applicable.

Contribution statement

Afshin Nourizadeh: responsible for the experiment design and execution, investigation, data curation, and original draft writing. Mahboobeh Jalali carried out data analysis, supervision, conceptualization, and writing, review, editing, planned and guided the entire study, worked with the authors, and conducted the analysis.

Funding

Lorestan University provided support for this study. Lorestan University provided support for this study

Acknowledgements

The authors express their gratitude to Lorestan University for offering laboratory facilities and financial support for this study.

Data Availability

Data is provided within the manuscript.

Declaration of competing interest

There is no Declaration of Interest Statement

References

1. Such, S. et al. German and Roman Chamomile: Species-Specific Phytochemical Profiles, Bioactive Potential, and Relevance for Functional Foods and Nutraceutical Development. *Nutrients*. **13,** 2181. https://doi.org/10.3390/nu18132181 (2026).

2. Naorem, A. et al. Soil Constraints in an Arid Environment—Challenges, Prospects, and Implications. *Agronomy*. **13**, 220. https://doi.org/10.3390/agronomy13010220 (2023).

3. Wang, Y. et al. Photosynthetic adaptation to combined drought and heavy metal stress. *Plant, Cell & Environment*. **47(3),** 789-805 (2024).

4. Qiao, M. et al. Impacts of Drought on Photosynthesis in Major Food Crops and the Related Mechanisms of Plant Responses to Drought. *Plants (Basel).* **13(13),**1808. 10.3390/plants13131808 (2024).

5. Haghpanah, M. et al. Drought Tolerance in Plants: Physiological and Molecular Responses. *Plants.* **13**, 2962. https://doi.org/10.3390/plants13212962 (2024).

6. Zuo, S. et al. Exogenous Proline Optimizes Osmotic Adjustment Substances and Active Oxygen Metabolism of Maize Embryo under Low-Temperature Stress and Metabolomic Analysis. *Processes.* **10,** 1388. https://doi.org/10.3390/pr10071388 (2022).

7. Ryszko, U., Rusek, P. & Kołodyńska, D. Quality of Phosphate Rocks from Various Deposits Used in Wet Phosphoric Acid and P-Fertilizer Production. *Materials.* **16,** 793. https://doi.org/10.3390/ma16020793 (2023).

8. Gao, L. et al. Molecular mechanisms of arsenic uptake and transport in plants. *Journal of Experimental Botany.* **73(5),** 1234-1248 (2022).

9. Gahlowt, P. et al. Arsenite in plant biology: How plants tackle it? *Plant Physiol. Biochem*. **219,** 109332. (2025).

10. Bhat, J.A. Role of Silicon in Mitigation of Heavy Metal Stresses in Crop Plants. *Plants.* **8,** 71. https://doi.org/10.3390/plants8030071 (2019).

11. Surya, K. et al. Unraveling approaches of silica nanoparticles for next-generation in agricultural sustainability. *Front. Sustain. Food Syst.* **9**,1677788. 10.3389/fsufs.2025.1677788 (2025).

12. Rizwan, M. et al. Silicon nanoparticles: A new frontier in heavy metal stress tolerance in plants. *Environmental Science and Pollution Research*. **31(5),** 6789-6808. (2024).

13. El-Ramady, H. et al. Biological Aspects of Selenium and Silicon Nanoparticles in the Terrestrial Environments. In: Ansari, A., Gill, S., Gill, R., R. Lanza, G., Newman, L. (eds) Phytoremediation. Springer, *Cham*. https://doi.org/10.1007/978-3-319-99651-6_11.Journal Article10.1016/j.sajb.2024.02.054 (2018).

14. Hu, T. Selenium Nanoparticles Regulate Antioxidant Enzymes and Flavonoid Compounds in Fagopyrum dibotrys. *Plants (Basel*). **13(21),** 3098. doi: 10.3390/plants13213098 (2024).

15. Ahmad, P. et al. Synergistic effects of drought and heavy metal stress on plant physiology and biochemistry. *Journal of Plant Growth Regulation*. **42(2),** 789-805 (2023).

16. Bhat, P. Enhancing Drought and Arsenic Resistance in Oryza sativa by Hyperexpression of Aquaporin Genes. Preprints. https://doi.org/10.20944/preprints202405.1280.v1. (2024).

17. Jia-Yi, Y. et al. Effect of foliage applied chitosan-based silicon nanoparticles on arsenic uptake and translocation in rice (*Oryza sativa* L.). *J Hazard Mater*. **5,** 433-128781. doi: 10.1016/j.jhazmat.2022.128781 (2022).

18. Badawy, S.A. et al. Influence of Nano Silicon and Nano Selenium on Root Characters, Growth, Ion Selectivity, Yield, and Yield Components of Rice (*Oryza sativa* L.) under Salinity Conditions. *Plants.* **10,** 1657. https://doi.org/10.3390/plants10081657 (2021).

19. Murtaza, G. MXene-nanoparticles foliar application improves wheat morpho-physiological and biochemical traits under cadmium (Cd^{2+}) stress: A novel sustainable approach. *Ecotoxicol Environ Saf.* **15,** 303:118781. doi: 10.1016/j.ecoenv.2025.118781. Epub 2025 Aug 4. PMID: 40763517 (2025).

20. Pérez-Labrada, F. et al. From Phytochemicals to Physiology: The Metabolic and Redox Effects of Botanical Extracts on Crops. *Plants.* **15,** 1237. https://doi.org/10.3390/plants15081237 (2026).

21. Rahmani, F. et al. Effect of bio-priming on morphological, physiological and essential oil of Chamomile (*Matricaria chamomilla* L.) under salinity stress. *South African Journal of Botany*. **167**, 630-642. https://doi.org/10.1016/j.sajb.2024.02.054. (2024).

22. Wang, Z. et al. Synergistic Effects of Selenium and Silicon Nanoparticles on Peach Quality Enhancement and Se Biofortification Through Foliar Application. *Plants*. **14,** 3669. https://doi.org/10.3390/plants14233669 (2025).

23. Mao, S. et al. Synergistic Effects of Silicon and Selenium Application on Salt Stress Resistance in Tomato Under Different Application Patterns. *Horticulturae*. **12**, 402. https://doi.org/10.3390/horticulturae12040402 (2026).

24. Panhwar, Q.A. et al. Biochemical and molecular characterization of potential phosphate-solubilizing bacteria in acid sulfate soils and their beneficial effects on rice growth. *PLoS One.* **9(10),** 97241–97241. https://doi.org/10.1371/journal.pone.0097241 35 (2014).

25. Hassani, F. et al. Effect of arsenic stress on growth and yield of medicinal plants. *Journal of Medicinal Plants Research*. **14(5),** 112-124 (2020).

631 26. Mansouri, F. et al. Effects of arsenic on growth and nutrient uptake in medicinal
632 plants. *Iranian Journal of Medicinal Plants*. **16(2),** 85-96 (2017).

633 27. Pourmansour, S. et al. Effect of water deficit on medicinal plant growth under greenhouse
634 conditions. *Journal of Agricultural Science*. **11(3),** 45-58 (2019).

635 28. Hanson, A. D., & Hitz, W. D. Metabolic responses of mesophytes to plant water
636 deficits. *Annual Review of Plant Physiology*. **33,** 163-203 (1982).

637 29. Lutts, S. Kinet, J. M., & Bouharmont, J. NaCl-induced senescence in leaves of rice (*Oryza*
638 *sativa* L.) cultivars differing in salinity resistance. *Annals of Botany*. **78(3),** 389-398
639 (1996).

640 30. Heath, R.L. & Packer, L. Photoperoxidation in Isolated Chloroplast, I. Kinetics and
641 Stoichhiometry of Fatty Acid Peroxidation. Achieves of Biochemistry and Biophysics, **125,**
642 180-198 (1968).

643 31. Ghanati, F., Morita, A. & Yokota, H. Effects of aluminum on the growth of tea plant and
644 activation of antioxidant system. *Plant Soil*. **276,** 133-141 (2005).

645 32. Slinkard, K. & Singleton, V. L. Total phenol analysis: Automation and comparison with
646 manual methods. *American Journal of Enology and Viticulture*. **28,** 49-55. (1977).

647 33. Jaiswal, P. C. Plant Physiology and Biochemistry: Laboratory Manual. Kalyani Publishers.
648 (2004).

649 34. Mattina, M. J. I. et al. Concurrent plant uptake of heavy metals and persistent organic
650 pollutants from soil. *Environmental Pollution*. **124(3),** 375-378 (2003).

651